Published in final edited form as:
Biomaterials. 2014 April ; 35(13): 4213–4222. doi:10.1016/j.biomaterials.2014.01.060.

Matrix Metalloproteinase 2-sensitive Multifunctional Polymeric Micelles for Tumor-specific Co-delivery of siRNA and Hydrophobic Drugs

Lin Zhu[a,b], **Federico Perche**[a], **Tao Wang**[a], and **Vladimir P Torchilin**[a,*]

[a]Center for Pharmaceutical Biotechnology & Nanomedicine, Northeastern University, Boston, Massachusetts 02115, United States

[b]Department of Pharmaceutical Sciences, Irma Lerma Rangel College of Pharmacy, Texas A&M University Health Science Center, Kingsville, Texas 78363, United States

Abstract

Co-delivery of hydrophilic siRNA and hydrophobic drugs is one of the major challenges for nanomaterial-based medicine. Here, we present a simple but multifunctional micellar platform constructed by a matrix metalloproteinase 2 (MMP2)-sensitive copolymer (PEG-pp-PEI-PE) via self-assembly for tumor-targeted siRNA and drug co-delivery. The micellar nanocarrier possesses several key features for siRNA and drug delivery, including (i) excellent stability; (ii) efficient siRNA condensation by PEI; (iii) hydrophobic drug solubilization in the lipid "core"; (iv) passive tumor targeting via the enhanced permeability and retention (EPR) effect; (v) tumor targeting triggered by the up-regulated tumoral MMP2; and (vi) enhanced cell internalization after MMP2-activated exposure of the previously hidden PEI. These cooperative functions ensure the improved tumor targetability, enhanced tumor cell internalization, and synergistic antitumor activity of co-loaded siRNA and drug.

1. Introduction

Small interfering RNA (siRNA) have shown therapeutic potential against numerous diseases, including cancer [1–3]. However, the efficiency of siRNA is significantly compromised by their poor stability, short circulation time, non-specific tissue distribution, and insufficient cellular transport [4]. Polyethylenimine (PEI), a cationic polymer, has been widely used in gene and siRNA delivery, due to its excellent transfection capability [5]. To improve the efficiency of siRNA delivery, we have synthesized a lipid-polymer, PEI(1800Da)-1,2-dioleoyl-sn-glycero-3-phosphoethanolamine(DOPE) (PEI-PE), which possesses the advantages of both PEI and DOPE [6, 7]. However, the high charge of PEI causes the non-selective electrostatic interaction between the nanocarriers and biological molecules or membranes, leading to low tumor targeting. Paclitaxel (PTX), on the other hand, is one of the most commonly used antineoplastic agents. However, its applications are

*Corresponding author: Vladimir P Torchilin, 140 The Fenway, Rm215, 360 Huntington Ave., Northeastern University, Boston, Massachusetts 02115, United States. Tel: +1 617.373.3206. Fax: +1 617.373.4201. v.torchilin@neu.edu.

Supplementary Data
Supplementary data related to this article can be found at https://

complicated by its low solubility, off-target toxicity and acquired drug resistance. Although various drug delivery systems have been developed, co-delivery of siRNA and hydrophobic drugs like PTX remains a challenge. Usually, because of their distinct physicochemical properties, siRNA and hydrophobic drugs are loaded into individual carriers for simultaneous administration. Since these molecules may not be delivered to the same cell, low synergistic effects are possible [8, 9]. To achieve the better synergistic effect, co-delivery of these molecules by the same carrier has been investigated [8–10]. However, the targeted co-delivery of siRNA and drug to tumor cells by the same nanocarrier is rare.

Matrix metalloproteinases (MMPs), especially MMP2, are known to be involved in cancer invasion, progression, and metastasis. The up-regulated MMP2 is considered as a biomarker for diagnostics and prognostics in many cancers, and also provides a strategy for tumor-targeted drug delivery via an enzyme-triggered mechanism [11]. In our previous studies, a synthetic octapeptide (GPLGIAGQ) has been used as a stimulus-sensitive linker in both liposomal [12] and micellar nanocarriers [13] for MMP2-triggered tumor targeting. In this study, to deliver siRNA and hydrophobic drugs, a simple but multifunctional micellar nanocarrier constructed by an MMP2-sensitive self-assembling copolymer, polyethylene glycol -peptide -polyethylenimine-1,2-dioleoyl-sn-glycero-3-phosphoethanolamine (PEG-pp-PEI-PE), was developed (Figure 1A). The MMP2-sensitive multifunctional micelles formed by the PEG-pp-PEI-PE conjugate were evaluated for co-delivery of siRNA and hydrophobic drugs in terms of their chemical and physicochemical properties, *in vitro* siRNA and drug delivery/co-delivery efficiency, *in vitro* gene down-regulation and anticancer activity, and *in vivo* co-delivery efficiency and tumor targeting.

2. Experimental Section

2.1. Materials

Polyethylene glycol 2000-N-hydroxysuccinimide ester (PEG2000-NHS) was purchased from Laysan Bio, Inc. (Arab, AL). 1,2-dioleoyl-sn-glycero-3-phosphoethanolamine (DOPE), 1,2-dioleoylsn- glycero-3-phosphoethanolamine-N-(lissamine rhodamine B sulfonyl) (ammonium salt) (Rh-PE), and 1,2-dioleoyl-sn-glycero-3-phosphoethanolamine-N-(glutaryl) (Glutaryl-PE) were purchased from Avanti Polar Lipids, Inc. (Alabaster, AL). Branched polyethylenimine (PEI) with a molecular weight of 1,800 and 25,000 Da were purchased from Polysciences, Inc (Warrington, PA). The BCA Protein Assay Reagent, N-hydroxysuccinimide (NHS), chloroform, dichloromethane (DCM) and methanol were purchased from Thermo Fisher Scientific (Rockford, IL). Ninhydrin Spray reagent, Molybdenum Blue Spray reagent, heparin sodium salt, and 1-Ethyl-3-[3-dimethylaminopropyl] carbodiimide hydrochloride (EDC) were purchased from Sigma-Aldrich Chemicals (St. Louis, MO). Human active MMP2 protein (MW 66,000 Da) and TLC plate (silica gel 60 F254) were from EMD Biosciences (La Jolla, CA). Dialysis tubing (MWCO 2,000 Da) was purchased from Spectrum Laboratories, Inc. (Houston, TX). Dulbecco's modified Eagle's medium (DMEM), penicillin streptomycin solution (PS) (100×), Hoechst 33342, LysoTracker® Green DND-26 and trypsin-EDTA were from Invitrogen Corporation (Carlsbad, CA). FBS was purchased from Atlanta Biologicals (Lawrenceville, GA). SDS-PAGE precast gel (**4–20%)** was purchased from Expedeon Ltd. (San Diego, CA). Ready Gel Zymogram Gel (10% polyacrylamide gel with gelatin), Zymogram Renaturation Buffer and Zymogram Development Buffer were purchased form Bio-Rad (Hercules, CA). Human non-small cell lung cancer A549 cells were from ATCC (Manassas, VA). A549 cells stably expressing copGFP were from Cell Biolabs (San Diego, CA). Hank's Balanced Salt Solution (HBSS) was from Mediatech (Manassas, VA). Ambion® RNase Cocktail™ was purchased from Life Technologies (Grand Island, NY). Ethidium bromide was from ICN Biomedicals (Aurora, OH). The MMP2-cleavable

(GPLGIAGQ) and uncleavable (GGGPALIQ) octapeptides were synthesized by the Tufts University Core Facility (Boston, MA).

The anti-GFP siRNA (5′-AAGUGGUAGAAGCCGUAGCdTdT-3′ antisense), the scramble siRNA (5′-CCGUATCGUAAGCAGTACTdTdT-3′ antisense) and anti-survivin siRNA (AGCGCAACCGGACGAAUCCdTdT antisense) were synthesized by Invitrogen.

The human non-small cell lung cancer (A549) cells, GFP expressing (copGFP A549) cells or cervical cancer (HeLa) cells were grown in complete growth media (DMEM supplemented with 50 U/mL penicillin, 50 μg/mL streptomycin and 10% FBS) at 37 °C at 5% CO_2. The pacilitaxel resistant non-small cell lung cancer (A549 T24) cells (kindly provided by Dr. Susan Horwitz, Albert Einstein College of Medicine, Bronx, NY) were maintained in the complete growth media containing 24 nM paclitaxel.

2.2. Synthesis, Purification and Characterization of PEG-pp-PEI-PE

Three steps are involved in the synthesis of PEG-pp-PEI-PE. First, Glutaryl-PE was activated with 20-fold molar excess of NHS/EDC for 2 hour, then reacted with branched PEI (1,800Da) (1:1, molar ratio) in chloroform in the presence of a trace amount of triethylamine at room temperature overnight [6]. The product PEI-PE was purified by dialysis (MWCO 3500 Da) against water for 48 hours and characterized by ^{1}H-NMR using D_2O and $CDCl_3$ as solvents.

Second, the MMP2-cleavable octapeptide (GPLGIAGQ) and PEG2000-NHS (1.2:1, molar ratio) were mixed and stirred in the carbonate buffer (pH 8.2) under nitrogen protection at 4°C overnight. The unreacted peptide was removed by dialysis (MWCO 2,000 Da) against distilled water. The product PEG2000-peptide (PEG-pp) was checked by RP-HPLC as described in a previous study [12].

Finally, PEG-pp was activated with NHS/EDC and reacted with PEI-PE (1:1, molar ratio) in the presence of triethylamine at room temperature overnight. The reaction mixture was dialyzed against water (MWCO 3500 Da) for 48 hours. The PEG-pp-PEI-PE was characterized by ^{1}H-NMR using D_2O and $CDCl_3$ as solvents. For synthesis of the uncleavable conjugate, the scramble peptide (GGGPALIQ) was used.

2.3. Particle Size, Zeta Potential and Morphology

The particle size of PEG-pp-PEI-PE micelles, PEG-pp-PEI-PE/siRNA, or PEG-pp-PEI-PE/PTX/siRNA was measured by dynamic light scattering (DLS) on a Coulter® N4-Plus Submicron Particle Sizer (Beckman Coulter). The zeta potential was measured in HBSS by Zeta Potentiometer (Brookhaven Instruments). The morphology was analyzed by transmission electron microscopy (TEM) (model XR-41B) (Advanced Microscopy Techniques, Danvers, MA) using negative staining with 1% phosphotungstic acid (PTA).

2.4. Determination of Critical Micelle Concentration (CMC)

The CMC was determined by fluorescence spectroscopy using pyrene as a hydrophobic fluorescent probe [13]. Briefly, pyrene chloroform solution was added to the testing tube at the final concentration of 8×10^{-5} M and dried on a freeze-dryer overnight. Then, the polymers in HBSS were added to the tubes at a 5-fold serial dilution (from 10^{-1} to 10^{-8} mg/mL) and incubated with shaking at room temperature for 24h before measurement. The fluorescence intensity was measured on an F-2000 fluorescence spectrometer (Hitachi, Japan) with the excitation wavelengths (λ_{ex}) of 337 nm (I_3) and 334nm (I_1) and an emission wavelength (λ_{em}) of 390 nm. The intensity ratio (I337/I334) was calculated and plotted

against the logarithm of the polymer concentration. The CMC value was obtained as the crossover point of the two tangents of the curves.

2.5. Cleavage Study of PEG-pp-PEI-PE by Human MMP2

One mg/mL of the polymer was incubated with active human MMP2 (5ng/μL) in pH 7.4 HBS containing 10mM $CaCl_2$ at 37°C overnight [13]. Three methods were used to analyze the cleavage of the peptide linker. For thin layer chromatography (TLC), the samples were run in chloroform/methanol (8:2, v/v) followed by Dragendorff's reagent staining. For size exclusion chromatography, the polymers and Rh-PE were dissolved in chloroform and dried to form a thin film. The Rh-PE was incorporated into the polymeric micelles via hydration with HBSS as an indicator for the micelle peak in chromatograms. After enzymatic digestion, the reaction mixture was applied on a Shodex KW-804 size exclusion column at the flow rate of 1 mL/min of water and detected by both UV (280 nm) and fluorescence detectors (λ_{ex} = 570nm, λ_{em} = 595nm) on a Hitachi HPLC system. The zeta potential of samples was also measured in HBSS to indicate the change of the charge.

2.6. Preparation of PEG-pp-PEI-PE/siRNA and PEG-pp-PEI-PE/PTX/siRNA Complexes

To prepare PEG-pp-PEI-PE/siRNA complexes, siRNA was mixed with PEG-pp-PEI-PE micelles in HBSS at various N/P ratios and incubated at room temperature for 20 min, allowing for siRNA complex formation. For co-loading of PTX and siRNA, PTX and PEG-pp-PEI-PE were dissolved in chloroform and dried to form the drug-polymer film, followed by hydration with HBSS using vortex. The unentrapped PTX was removed by filtration through a 0.45μm filter (GE Healthcare) [7]. The PTX in filtrate was measured on a reversed-phase C_{18} column (250 mm×4.6 mm) using an isocratic mobile phase of acetonitrile and water (60:40, v/v) at a flow rate of 1.0 mL/min and detected at UV 227 nm on a Hitachi HPLC system. The PTX-loaded micelles were incubated with siRNA in HBSS at room temperature for 20 min. Then, the particle size, zeta potential and morphology of the complexes were analyzed.

2.7. Gel Retardation Assay

To confirm the siRNA complex formation, 0.4 μg of free siRNA or siRNA complexes (N/P 10, 20 and 40) were applied on a 2% pre-cast agarose gel containing ethidium bromide. The gel was run on an E-Gel® system (Invitrogen) for 15 min.

2.8. RNase Protection Assay

The resistance to nuclease digestion was determined using an RNase protection assay. The samples containing 0.4 μg of siRNA were incubated with 0.48 units of Ambion® RNase Cocktail™ for 2h at 37 °C. The RNase was then inactivated by 20 mM EDTA before complex dissociation using 2 mg/mL of dextran sulfate (500 kDa) for 20 min at 37 °C. Then, samples were analyzed on a 2% pre-cast agarose gel containing ethidium bromide.

2.9. Ethidium Bromide Exclusion Assay

The siRNA complexes were incubated with 12 μg/mL of ethidium bromide. The recovery of siRNA from their complexes was assessed by the fluorescence intensity after dissociation with heparin at 10 units per μg of siRNA. The fluorescence intensity was measured at λ_{ex} = 530 nm and λ_{em} = 640 nm on a microplate reader (Synergy HT, Biotek).

2.10. Protein Adsorption/Interaction

To evaluate the blood protein adsorption/interaction, the nanoparticles (PEG-pp-PEI-PE/PTX/siRNA) were incubated with the normal mouse serum (1:10, v/v) at 37°C for 12h. The particle size was analyzed by DLS on a Coulter® N4-Plus Submicron Particle Sizer.

2.11. In Vitro Drug Release

The PTX release rate from the PEG-pp-PEI-PE/PTX/siRNA was studied by a dialysis method. Briefly, the PEG-pp-PEI-PE/PTX/siRNA (0.4mL) was dialyzed (MWCO 2,000 Da) against 40 mL of water containing 1M sodium salicylate to maintain the sink condition [13] at 37°C. The PTX in the outside media was determined by RP-HPLC during the experiment.

2.12. In Vitro Cellular Uptake

To study the cellular uptake, A549 cells were seeded in 24-well plates at 1.6×10^5 cells/well 24 h before experiments. To study the influence of the MMP2 on the cellular uptake, the FAM-siRNA was used to prepare the siRNA polyplexes at N/P 40. The cells were washed and replaced with serum-free media. The siRNA polyplexes were added to cell media and incubated with cells for 1h. To test the cellular uptake of the siRNA polyplexes without MMP2 pretreatment, the siGLO siRNA was used as an indicator. The siGLO siRNA polyplexes (N/P40) were incubated with cells in complete growth media for 4h. To evaluate the *in vitro* co-delivery efficiency, the Oregon green PTX and siGLO siRNA were used to prepare the nanoparticles. The nanoparticles were incubated with the cells in complete growth media for 2h.

Then, the media was removed and the cells were washed with serum-free media three times. For FACS analysis, the cells were trypsinized and collected by centrifugation at 2,000 rpm for 4 min. After washing with ice-cold PBS, the cells were re-suspended in 400μL of PBS and applied on a BD FACS Calibur flow cytometer (BD Biosciences). The cells were gated upon acquisition using forward versus side scatter to exclude debris and dead cells. The data was collected (10,000 cell counts) and analyzed with BD Cell Quest Pro Software. For confocal microscopy, the cells were fixed by 4% paraformaldehyde (PFA). To visualize cell nuclei, cells were stained with 5μM of Hoechst 33342 for 15min at RT. To indicate the endosome, cells were stained with LysoTracker® Green DND-26. The photos were taken with a Zeiss LSM 700 confocal microscope system at 63× magnification and analyzed using Zeiss Image Browser software.

2.13. Gene Down-regulation

The copGFP A549 or A549 T24 cells were seeded at 5×10^4 cells/well in 24 well culture plates 24h before transfection. The anti-GFP siRNA polyplexes (N/P40) were incubated with copGFP A549 cells in complete growth media for 48 h (one tranfection) or for 3 transfections (every other day). The cells were collected and analyzed by flow cytometry. After 3 transfections, the cells were also pictured by confocal microscopy. To down-regulate the survivin protein, the PEG-pp-PEG-PE/anti-survivin siRNA complexes were incubated with A549 T24 cells for 48 h. Then the cells were collected and lysed. The total survivin in cell lysates was determined by a human total survivin immunoassay kit and normalized by the total protein concentration determined by the BCA protein assay.

2.14. Cytotoxicity Study

To study the toxicity of the polymers, A549 or HeLa cells were seeded at 4000 cells/well in 96-well plates 24h before treatments. A series of diluted polymer (PEI 1800Da or PEG-pp-PEI-PE) solutions were added to cells and incubated for 72h. To study the toxicity of the siRNA polyplexes, the siRNA polyplexes with various N/P ratios were added to cells and incubated for 72h.

To study the cytotoxicity of PTX, PEG-pp-PEI-PE/PTX or PEG-pp-PEI-PE/PTX/siRNA, A549 or A549 T24 cells were seeded at 2000 cells/well in 96-well plates 24h before treatments. The PTX or its formulations were incubated with the cells for 72h in complete

growth media. The cell viability was determined by Cell Titer-Blue® Cell Viability Assay. Briefly, 15 μL of CellTiter-Blue® Reagent was diluted with 100 μL of complete growth medium per well and incubated with treated cells at 37°C for 2h. Thereafter, the fluorescence intensity was recorded at λ_{ex}=560nm and λ_{em}=590nm using a Labsystems Multiskan MCC/340 microplate reader.

2.15. In Vivo Co-delivery of PTX and siRNA

Female nude mice (NU/NU, 4–6 weeks old) were purchased from Charles River laboratories (Wilmington, MA). All animal procedures were performed according to an animal care protocol approved by Northeastern University Institutional Animal Care and Use Committee. Approximately 5×10^6 A549 cells suspended in 50μl HBSS were mixed with the phenol-red free high concentration Matrigel™ (1:1, v/v) and inoculated in nude mice by subcutaneous injection over their right flanks. The tumor was monitored for length (l) and width (w) by caliper and calculated by the equation $V=lw^2/2$.

HBSS, the MMP2-sensitive PEG-pp-PEI-PE/Oregon green PTX/siGLO siRNA complexes and their nonsensitive counterparts were intravenously injected in tumor-bearing mice with a tumor size of about 400 mm^3 via tail vein. At 2 h post-injection, mice were anesthetized and sacrificed. The tumor and major organs (heart, liver, spleen, lung, and kidney) were collected. The fresh tissues were minced into small pieces and incubated in 400 U/mL of collagenase D solution for 30 min at 37°C to dissociate cells [14]. The single-cell suspension was analyzed immediately by FACS.

2.16. Statistical Analysis

Data were presented as mean ± standard deviation (SD). The difference between the groups was analyzed using a one-way ANOVA analysis by the commercial software PASW® Statistics 18 (SPSS). $P < 0.05$ was considered statistically significant.

3. Results and Discussion

3.1. Synthesis and Characterization of PEG-pp-PEI-PE

The three-step synthesis of PEG-pp-PEI-PE is shown in the Figure S1. In our previous work, PEG2000-peptide [13] and PEI-PE [6, 7] have been successfully synthesized. Here, the same methods were used. Then, PEG-pp was conjugated with PEI-PE in the presence of the coupling reagents (NHS/EDC). Figure 1B shows the ^{1}H-NMR spectra of PEG-pp-PEI-PE. In $CDCl_3$, the characteristic peaks of PEG-pp-PEI-PE were displayed [DOPE(-CH_2-), 0.6~1.8 ppm; PEI(-CH_2CH_2NH-), 1.8~3 ppm; PEG (-CH_2CH_2O-), 3.60~3.65 ppm]. However, most peaks of PE were disappeared or significantly lowered when D_2O was used as solvent. This could be due to the formation of “core-shell” nanostructure in which the hydrophobic PE (and adjacent PEI) was entrapped in its “core” and isolated by the hydrophilic PEG “shell” in water, whereas the polymer would be fully dissolved in chloroform. The similar phenomenon was observed in the ^{1}H-NMR spectra of the intermediate PEI-PE (Figure S2). The integration of the characteristic peaks indicated that the molar ratio between PEG, PEI and PE was about 1:1:1.

3.2. Micelle Formation and MMP2 sensitivity

To confirm the micelle formation of PEG-pp-PEI-PE, the critical micelle concentration (CMC) (Figure 1C) and particle size (Figure 1D) were measured. The CMC of PEG-pp-PEI-PE was about 2.04×10^{-7} M, which is in the range of the CMC of the PEG-lipid micelles [15], indicating the formation of a micellar nanostructure. The PEG-pp-PEI-PE micelles were small and uniform and their particle size was consistent in a broad range of pH from 5.5 to 9.0, indicating the excellent stability of their micellar nanostructure.

The MMP2 sensitivity of PEG-pp-PEI-PE was determined by enzymatic digestion followed by thin layer chromatography, size exclusion HPLC and zeta potential measurement. The MMP2 cleaved PEG-pp-PEI-PE at the site between glycine (G) and isoleucine (I) [12], resulting in two fractions. The released PEG moiety (PEG-GLPG) was visualized as a new spot on the TLC plate while the PEI-PE moiety (IAGQ-PEI-PE) could not move due to its high polarity (Figure 2A). In the size exclusion chromatogram (Figure 2B), the peaks of micelles formed by PEI-PE or PEG-pp-PEI-PE were indicated by fluorescent Rh-PE (red, discontinuous) due to the strong binding force between the Rh-PE and hydrophobic core of the micelles. After MMP2 treatment, the peak of PEG-GLPG was shown with a longer retention time but without fluorescence signal, while the IAGQ-PEI-PE was still form the micellar nanostructure as evidenced by the overlay between the UV and fluorescence signal. The data indicated that the PEG was released from the micelles and the micellar nanostructure was still remained after MMP2 cleavage. The stable micellar nanostructure ensures the high hydrophobic drug loading and low drug leakage before and after MMP2 cleavage in the *in vitro* and *in vivo* conditions.

As expected, conjugation of PEG-pp to PEI-PE significantly decreased the zeta potential of the formed conjugate from 50.7±4.2 to 26.8±2.4 mV, while no decrease in the zeta potential was observed by mixing of PEI-PE with PEG-pp (53.6±1.3 mV), supporting that only covalent conjugation between PEG-pp and PEI-PE could shield the positive charge of PEI. In contrast, the MMP2 cleavage removed the PEG corona from the micelles and exposed PEI resulting in an increase in the zeta potential (50.2±1.1 mV) (Figure 2C).

3.3. Preparation and Characterization of siRNA and PTX Loaded Micelles

Free siRNA could be completely condensed by PEG-pp-PEI-PE at a nitrogen to phosphate ratio (N/P) of 40 (Figure S4) and be protected thereafter from RNase degradation (Figure S5). The condensed siRNA however could be dissociated from the siRNA complexes by negatively charged heparin, ensuring the efficient siRNA release upon cell entry (Figure S6).

The poorly water-soluble PTX was loaded into the lipid core of the micelles via the hydrophobic interaction. The final drug loading was about 2.3 wt%, which was in agreement with the previous reports [15]. In the “sink condition”, only about 20% of the loaded PTX was released from PEG-pp-PEI-PE/PTX/siRNA complexes after 4h incubation, while more than 80% drug was released after 20h incubation (Figure S7). This appropriate drug release profile ensured the efficient cell internalization of the loaded PTX as well as the sufficient dose of the released PTX for effective anticancer activity after endocytosis. The particle size of PEG-pp-PEI-PE/PTX/siRNA complexes was about 43nm and wasn’t increased much compared to that of PEG-pp-PEI-PE/siRNA complexes (about 37nm) (Figure 3A). They were much smaller than PEI/siRNA complexes (about 340nm), probably due to their uniform “core-shell” nanostructure and less aggregation (Figure 3B and 3C). The zeta potential of PEG-pp-PEI-PE/PTX/siRNA nanoparticles was neutral (Figure 3D), which is appropriate for *in vivo* nucleic acid delivery [5]. It was notable that the size of PEG-pp-PEI-PE/siRNA or PEG-pp-PEI-PE/PTX/siRNA didn’t change significantly before and after MMP2 cleavage and was similar to that of PEI-PE/siRNA, suggesting that PEG-pp-PEI-PE/PTX/siRNA complexes would be fairly stable during *in vivo* MMP2 cleavage in the tumor microenvironment (Figure 3A).

To estimate the *in vivo* blood protein adsorption/interaction, PEG-pp-PEI-PE/PTX/siRNA nanoparticles were diluted by the mouse serum. In the presence of high content of serum, the fraction of large aggregates (≥1000nm) caused by the interaction of PEG-pp-PEI-PE/PTX/siRNA and serum proteins was not significantly increased after 4h incubation at 37°C while just slightly increased from 0.8% to 1.7% after 12h incubation (Figure 3E). That’s probably

due to high density of PEG and appropriate PEG length on the surface of nanoparticles [13, 16]. The PEG-pp-PEI-PE/PTX/siRNA nanoparticles with the minimized blood protein adsorption and small size are more likely to "escape" the capture by immune cells [16].

The sufficient drug loading, easy preparation procedure, small and uniform size, neutral charge, excellent stability, and negligible blood protein adsorption ensure the PEG-pp-PEI-PE micelles as an excellent platform for co-delivery of siRNA and hydrophobic drugs.

3.4. *In vitro* Cellular Uptake

To study the influence of MMP2 on the cellular uptake of siRNA/polymer complexes, the PEG-pp-PEI-PE/siRNA complexes were pretreated with MMP2 before incubation with non-small cell lung cancer (NSCLC) cells (A549) in the serum-free medium. The cellular uptake of PEG-pp-PEI-PE/siRNA was significantly increased from 400%(**c**) to 650% (**d**) after MMP2 cleavage, the level similar to that of PEI-PE/siRNA (Figure 4A), due to the PEG de-shielding and full exposure of PEI.

Without MMP2 pretreatment, PEG-pp-PEI-PE/siRNA showed higher transfection efficiency than that of the "gold standard" of transfection reagents, branched high molecular weight PEI (25K Da), while its uncleavable counterpart didn't show significant transfection (Figure 4B). The data indicated that the extracellular MMP2 in cancer cell media was sufficient to cleave the peptide linker [13] and the culture serum (protein) had little effect on the cell internalization of PEG-pp-PEI-PE/siRNA. However, their transfection efficiency was still lower than that of PEI-PE/siRNA, probably due to the strong interaction between the positively charged PEI-PE/siRNA and cell membrane. This is understandable. The N/P 40 used for preparation of PEI-PE/siRNA was much higher than the needed value (N/P<10) to condense siRNA (Figure S4), resulting in "extra positive charge" on the PEI-PE/siRNA complexes, while the zeta potential of PEG-pp-PEI-PE/siRNA was around neutral. From an *in vivo* point of view, high positive charge may cause the non-specific biodistribution and toxicity [5] and the near-neutral nanoparticles are preferred. The cellular uptake of the siRNA complexes was confirmed by confocal microscopy (Figure 4C). Furthermore, the colocalization of siRNA (red) and the endosome/lysosome (green) indicated that the siRNA complexes most likely underwent endocytic pathway upon cell entry. The components (PEI and DOPE) of PEG-pp-PEI-PE were designed to facilitate the endosomal escape [5] and the following successful RNAi.

To estimate the *in vitro* co-delivery efficiency, the Oregon green-PTX and siGLO siRNA were co-loaded into PEG-pp-PEI-PE micelles. Compared to PEI25k which could only deliver siRNA but not PTX into cells, both MMP2 sensitive and nonsensitive PEG-pp-PEI-PE micelles were capable of co-delivery of siRNA and PTX. However, compared to the nonsensitive counterparts (69.8%), MMP2-sensitive micelles co-delivered siRNA and PTX to almost all cells (98.2%), a result of the MMP2-induced PEG de-shielding and PEI exposure (**dot plot,** Figure 5A). The fluorescence intensity in the MMP2-sensitive micelle-treated cells was much higher than those in the nonsensitive micelle-treated ones (siRNA: 93.6% vs. 44.7%, PTX: 137.5% vs. 82.4%) (**histogram**, Figure 6A). The co-delivery/colocalization of PTX and siRNA was further confirmed by the orange-yellow dots in the merged image under confocal microscopy (Figure 5B).

3.5. Gene Down-regulation

To study the gene down-regulation of the anti-GFP siRNA, the GFP expressing (copGFP A549) cells were used as a cell model. In the presence of serum, one transfection of PEG-pp-PEI-PE/anti-GFP siRNA brought down the GFP expression to about 45% (**b**) of that of untreated cells (**e**), which was comparable to those of non-PEGylated siRNA complexes (**a**)

and PEI 25K/siRNA complexes. In contrast, the nonsensitive siRNA complexes (**c**) didn't show any GFP down-regulation. Three transfections led to more significant GFP down-regulation compared to one transfection (Figure 6A). The data was confirmed by confocal microscopy as evidenced by the loss of the green fluorescence (Figure 6B). It was notable that PEI25K induced high gene down-regulation although its cellular uptake efficiency was not higher than PEI-PE or PEG-pp-PEI-PE (Figure 4), probably due to its excellent buffering capacity-induced endosomal escape [5].

Besides, the therapeutic siRNA was used to evaluate the performance of PEG-pp-PEI-PE. Survivin, an inhibitor protein of apoptosis, is found up-regulated in malignant tumors, especially in drug resistant cells [17]. Anti-survivin siRNA have been used to down-regulate survivin and potentiate the anticancer activity of chemotherapeutics [18]. Here, an anti-survivin siRNA was complexed with PEG-pp-PEI-PE and transferred into PTX-resistant (A549 T24) NSCLC cells in the presence of serum. The survivin protein was down-regulated for about 30% at 150nM siRNA and the down-regulation effect was dose-dependent (Figure 6C). However, compared to the reporter gene, down-regulation of the therapeutic gene was relatively tough [19]. The similar gene down-regulation level by the survivin siRNA was observed in the previous study [20, 21].

3.6. *In Vitro* Synergistic Effect

To study the synergistic effect of the anti-survivin siRNA and PTX co-loaded nanocarrier, both PTX -sensitive (A549) and -resistant (A549 T24) NSCLC cells were used. Compared to A549 cells with the IC50 of about 5.2 nM PTX, the A549 T24 cells were more resistant to PTX as evidenced by its high IC50 of about 96 nM PTX (Figure S9) Incubation of PEG-pp-PEI-PE/PTX with A549 or A549 T24 cells significantly increased the cytotoxicity of PTX compared to those of free PTX or its nonsensitive micelles (Figure 7A), probably due to the increased drug solubility and enhanced cellular uptake (Figure 5). Furthermore, the simultaneous delivery of anti-survivin siRNA and PTX significantly brought down the IC50 of PTX to about 15nM (Figure 7B). In contrast, the polymer itself or complexed with siRNA are very safe (Figure S8) and no any cytotoxicity of anti-survivin siRNA at the used doses was observed (Figure S10). Altogether, this enhanced antitumor activity was a result of the enhanced co-delivery efficiency and synergistic effect of PTX and anti-survivin siRNA [22].

3.7. *In Vivo* Co-delivery of siRNA and PTX

The *in vivo* co-delivery efficiency was studied on a NSCLC xenograft mouse model. Two hour after *i.v.* injection, siGLO siRNA and Oregon green PTX were predominately accumulated in tumor tissues and internalized by tumor cells, as evidenced by the high fluorescence of both siRNA and PTX in the tumor cells. In contrast, no obvious cell internalization of the fluorescent PTX or siRNA was observed in the major organs (Figure 8A). The data indicated that PEG-pp-PEI-PE micelles were capable of targeted delivery of their payloads to the tumor via both the enhanced permeability and retention (EPR) effect and MMP2 sensitivity. The MMP2-mediated cleavage de-shielded PEG and exposed PEI, leading to the enhanced tumor cell internalization of the nanoparticles. In the tumor, about 14.4% of total cells internalized both siRNA and PTX after administration of PEG-pp-PEI-PE/PTX/siRNA. It was about 2.4-fold higher than that of its nonsensitive counterpart (6%) (Figure 8B). The *in vivo* co-delivery efficiency was lower than the *in vitro* data (Figure 5), which was in agreement with previous studies [9]. Unlike the *in vitro* condition, the *in vivo* condition is more complicated and many factors including non-specific tissue distribution [13], extracellular drug accumulation [13, 23], and limited tissue penetration [24, 25], influence the tumor cell internalization of drug and siRNA. Other factors such as low doses and non-optimized time of sampling also play an important role in the *in vivo* drug delivery.

The optimization of dose regimen for *in vivo* drug delivery and antitumor efficacy study are undergoing.

4. Conclusion

We successfully synthesized an MMP2-sensitive self-assembling block co-polymer, PEG-pp-PEI-PE. The micellar nanocarriers constructed by this polymer via self-assembly possessed several key features for siRNA and drug delivery, including (i) excellent stability; (ii) efficient siRNA condensation by PEI; (iii) hydrophobic drug solubilization in the lipid "core"; (iv) passive tumor targeting via the EPR effect; (v) tumor targeting triggered by the up-regulated tumoral MMP2; and (vi) enhanced cell internalization after MMP2-activated exposure of the previously hidden PEI. These cooperative functions improved the tumor targeting, tumor cell internalization, and synergistic antitumor activity of co-loaded siRNA and hydrophobic drugs. This multifunctional drug delivery platform showed great potential for cancer cell-selective co-delivery of siRNA and anticancer drugs.

Supplementary Material

Refer to Web version on PubMed Central for supplementary material.

Acknowledgments

This work was supported by the NIH Grants 1R01CA121838 and U54CA151881 to Dr. Vladimir P. Torchilin and also supported in part by a Postdoctoral Fellowship (PF-13-361-01-CDD) from American Cancer Society-Ellison Foundation to Dr. Lin Zhu. The authors thank Dr. Rupa Sawant, Mr. Anton Taigind, and Mr. Amey Kanitkar for their kind help during this study.

References

1. Song E, Lee SK, Wang J, Ince N, Ouyang N, Min J, et al. RNA interference targeting Fas protects mice from fulminant hepatitis. Nat Med. 2003; 9:347–51. [PubMed: 12579197]
2. de Fougerolles A, Vornlocher HP, Maraganore J, Lieberman J. Interfering with disease: a progress report on siRNA-based therapeutics. Nat Rev Drug Discov. 2007; 6:443–53. [PubMed: 17541417]
3. Oh YK, Park TG. siRNA delivery systems for cancer treatment. Adv Drug Deliv Rev. 2009; 61:850–62. [PubMed: 19422869]
4. De Paula D, Bentley MV, Mahato RI. Hydrophobization and bioconjugation for enhanced siRNA delivery and targeting. Rna. 2007; 13:431–56. [PubMed: 17329355]
5. Zhu L, Mahato RI. Lipid and polymeric carrier-mediated nucleic acid delivery. Expert Opin Drug Deliv. 2010; 7:1209–26. [PubMed: 20836625]
6. Sawant RR, Sriraman SK, Navarro G, Biswas S, Dalvi RA, Torchilin VP. Polyethyleneimine-lipid conjugate-based pH-sensitive micellar carrier for gene delivery. Biomaterials. 2012; 33:3942–51. [PubMed: 22365809]
7. Navarro G, Sawant RR, Biswas S, Essex S, Tros de Ilarduya C, Torchilin VP. P-glycoprotein silencing with siRNA delivered by DOPE-modified PEI overcomes doxorubicin resistance in breast cancer cells. Nanomedicine (Lond). 2012; 7:65–78. [PubMed: 22191778]
8. Wang Y, Gao S, Ye WH, Yoon HS, Yang YY. Co-delivery of drugs and DNA from cationic core-shell nanoparticles self-assembled from a biodegradable copolymer. Nat Mater. 2006; 5:791–6. [PubMed: 16998471]
9. Sun TM, Du JZ, Yao YD, Mao CQ, Dou S, Huang SY, et al. Simultaneous delivery of siRNA and paclitaxel via a "two-in-one" micelleplex promotes synergistic tumor suppression. ACS nano. 2011; 5:1483–94. [PubMed: 21204585]
10. Chen AM, Zhang M, Wei D, Stueber D, Taratula O, Minko T, et al. Co-delivery of doxorubicin and Bcl-2 siRNA by mesoporous silica nanoparticles enhances the efficacy of chemotherapy in multidrug-resistant cancer cells. Small. 2009; 5:2673–7. [PubMed: 19780069]

11. Zhu L, Torchilin VP. Stimulus-responsive nanopreparations for tumor targeting. Integr Biol. 2013; 5:96–107.
12. Zhu L, Kate P, Torchilin VP. Matrix metalloprotease 2-responsive multifunctional liposomal nanocarrier for enhanced tumor targeting. ACS nano. 2012; 6:3491–8. [PubMed: 22409425]
13. Zhu L, Wang T, Perche F, Taigind A, Torchilin VP. Enhanced anticancer activity of nanopreparation containing an MMP2-sensitive PEG-drug conjugate and cell-penetrating moiety. Proc Natl Acad Sci USA. 2013; 110:17047–52. [PubMed: 24062440]
14. Kortylewski M, Kujawski M, Wang T, Wei S, Zhang S, Pilon-Thomas S, et al. Inhibiting Stat3 signaling in the hematopoietic system elicits multicomponent antitumor immunity. Nat Med. 2005; 11:1314–21. [PubMed: 16288283]
15. Lukyanov AN, Torchilin VP. Micelles from lipid derivatives of water-soluble polymers as delivery systems for poorly soluble drugs. Adv Drug Deliv Rev. 2004; 56:1273–89. [PubMed: 15109769]
16. Walkey CD, Olsen JB, Guo H, Emili A, Chan WC. Nanoparticle size and surface chemistry determine serum protein adsorption and macrophage uptake. J Am Chem Soc. 2012; 134:2139–47. [PubMed: 22191645]
17. Ambrosini G, Adida C, Altieri DC. A novel anti-apoptosis gene, survivin, expressed in cancer and lymphoma. Nat Med. 1997; 3:917–21. [PubMed: 9256286]
18. Altieri DC. Survivin, versatile modulation of cell division and apoptosis in cancer. Oncogene. 2003; 22:8581–9. [PubMed: 14634620]
19. Zhu L, Mahato RI. Targeted delivery of siRNA to hepatocytes and hepatic stellate cells by bioconjugation. Bioconjug Chem. 2010; 21:2119–27. [PubMed: 20964335]
20. Li S-D, Huang L. Targeted delivery of antisense oligodeoxynucleotide and small interference RNA into lung cancer cells. Mol Pharm. 2006; 3:579–88. [PubMed: 17009857]
21. Salzano G, Riehle R, Navarro G, Perche F, De Rosa G, Torchilin VP. Polymeric micelles containing reversibly phospholipid-modified anti-survivin siRNA: A promising strategy to overcome drug resistance in cancer. Cancer Lett. 2014; 343:224–31. [PubMed: 24099916]
22. Shen J, Yin Q, Chen L, Zhang Z, Li Y. Co-delivery of paclitaxel and survivin shRNA by pluronic P85-PEI/TPGS complex nanoparticles to overcome drug resistance in lung cancer. Biomaterials. 2012; 33:8613–24. [PubMed: 22910221]
23. Kirpotin DB, Drummond DC, Shao Y, Shalaby MR, Hong K, Nielsen UB, et al. Antibody targeting of long-circulating lipidic nanoparticles does not increase tumor localization but does increase internalization in animal models. Cancer Res. 2006; 66:6732–40. [PubMed: 16818648]
24. Zorko M, Langel U. Cell-penetrating peptides: mechanism and kinetics of cargo delivery. Adv Drug Deliv Rev. 2005; 57:529–45. [PubMed: 15722162]
25. Cabral H, Matsumoto Y, Mizuno K, Chen Q, Murakami M, Kimura M, et al. Accumulation of sub-100 nm polymeric micelles in poorly permeable tumours depends on size. Nat Nanotechnol. 2011; 6:815–23. [PubMed: 22020122]

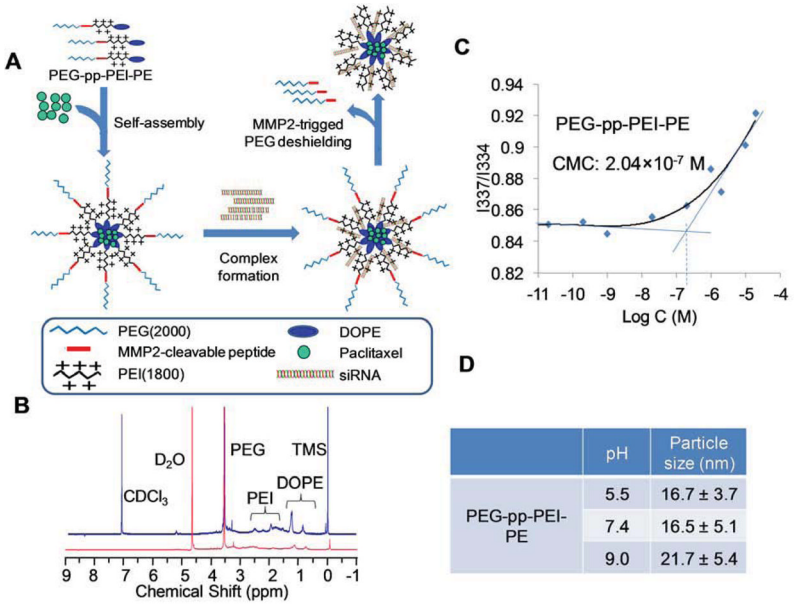

	pH	Particle size (nm)
PEG-pp-PEI-PE	5.5	16.7 ± 3.7
	7.4	16.5 ± 5.1
	9.0	21.7 ± 5.4

Figure 1.

(A) Drug delivery strategy; (B) ^{1}H-NMR in $CDCl_3$ (blue) and D_2O (red) of PEG-pp-PEI-PE; (C) Critical micelle concentration (CMC) of PEG-pp-PEI-PE micelles determined by fluorescence spectroscopy using pyrene as a fluorescent probe; (D) Particle size of PEG-pp-PEI-PE micelles at different pHs.

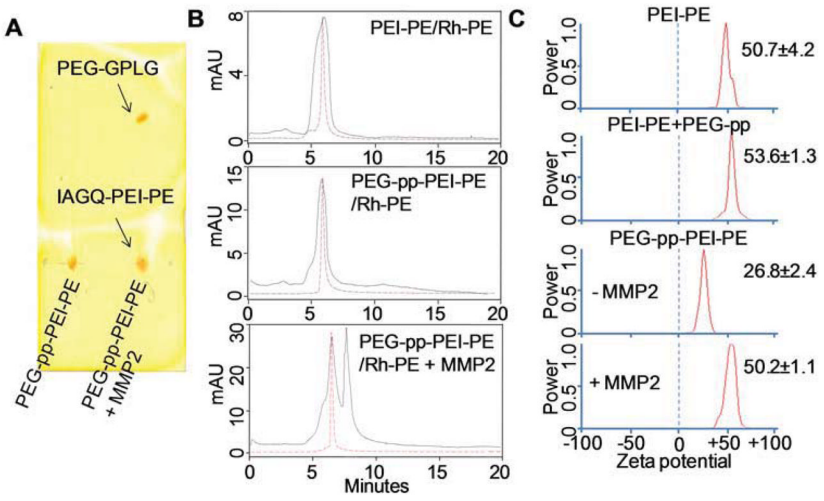

Figure 2.

Enzymatic cleavage of PEG-pp-PEI-PE (5ng/μL MMP2, overnight). (A) Thin layer chromatography; (B) The Rh-PE incorporated PEG-pp-PEI-PE micelles were digested and analyzed by size exclusion-HPLC. The fluorescence of Rh-PE was indicated by the red discontinuous curve. (C) Zeta potential of the polymers.

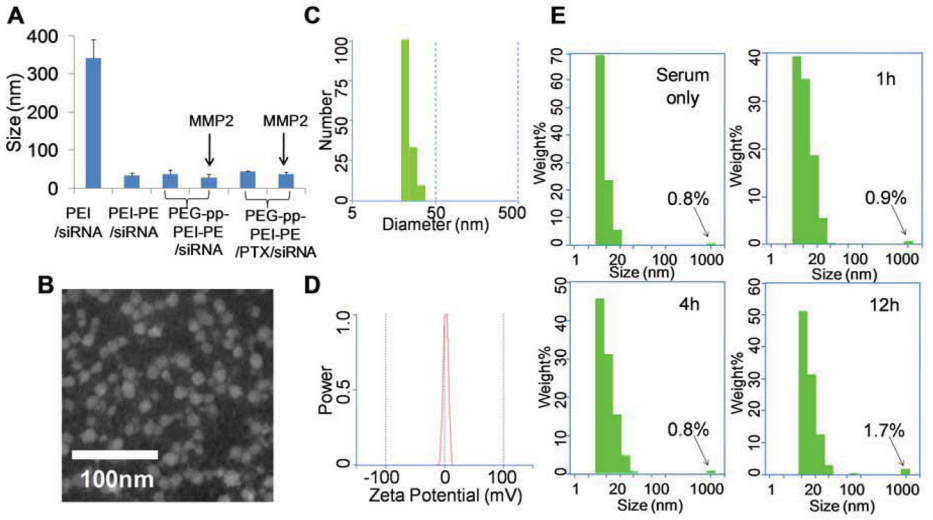

Figure 3.

Characterization of PTX and siRNA co-loaded PEG-pp-PEI-PE micelles. (A) Particle size of nanoparticles determined by DLS; (B) Transmission electron microscopy (TEM) of PEG-pp-PEI-PE/PTX/siRNA by negative staining with 1% PTA; (C) Particle size distribution of PEG-pp-PEI-PE/PTX/siRNA; (D) Zeta potential of PEG-pp-PEI-PE/PTX/siRNA; (E) Stability of PEG-pp-PEI-PE/PTX/siRNA in the serum (1:10, v/v) at 37°C.

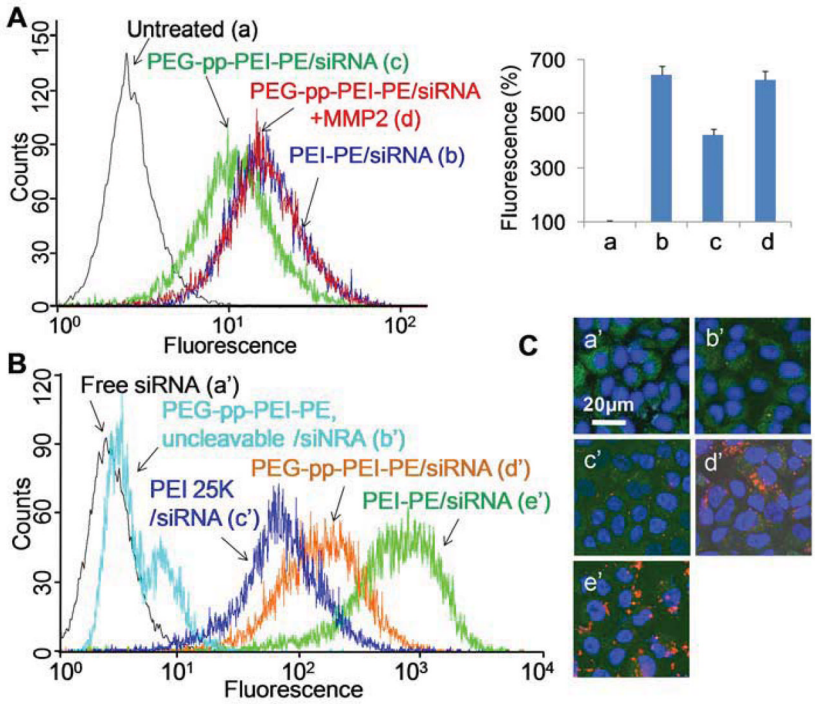

Figure 4.

In vitro cellular uptake of PEG-pp-PEI-PE/siRNA. (A) Cellular uptake after MMP2 pretreatment (1h incubation in serum-free medium); (B) Cellular uptake without MMP2 pretreatment (4h incubation in 10% FBS); (C) Confocal microscopy (4h incubation in 10% FBS). Cells were stained by Hoechst 33342 and LysoTracker® Green DND-26.

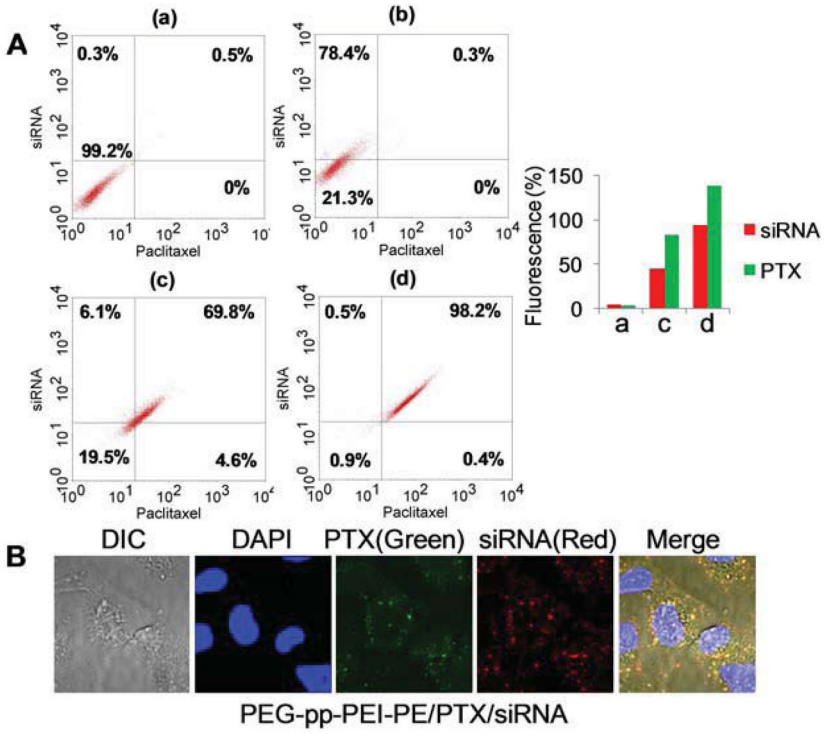

Figure 5.

In vitro co-delivery of siRNA and PTX. The nanoparticles loaded with Oregon green-PTX and siGLO siRNA were incubated with A549 cells in complete growth media for 2h. (A) FACS analysis. The siRNA and PTX co-delivered cells were indicated in the upper right quadrant. (a), untreated cells; (b), PEI25K/PTX/siRNA; (c), PEG-pp-PEI-PE uncleavable/PTX/siRNA; (d), PEG-pp-PEI-PE/PTX/siRNA. (B). Confocal microscopy. To visualize cell nuclei, the cells were stained by Hoechst 33342.

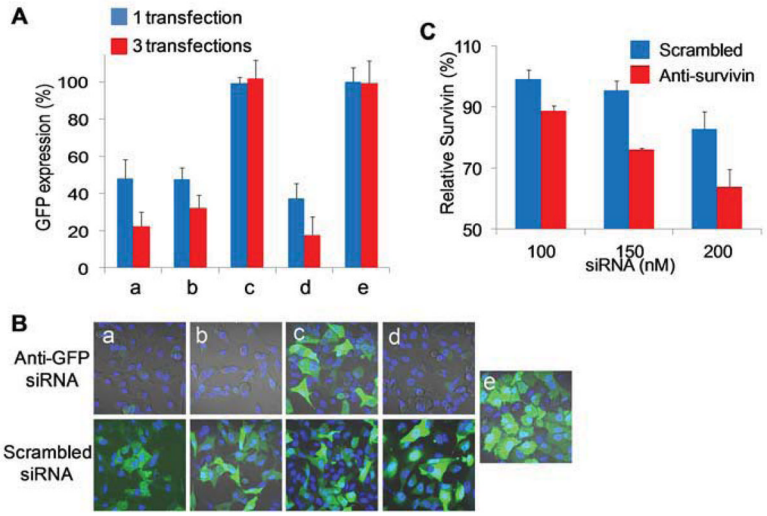

Figure 6.

Gene down-regulation study. (A) GFP down-regulation in copGFP A549 cells after one (blue) or three (red) transfections of PEG-pp-PEI-PE/anti-GFP siRNA; (B) GFP down-regulation analyzed by confocal microscopy after three transfections of anti-GFP siRNA complexes. a, PEI-PE/siRNA; b, PEG-pp-PEI-PE/siRNA; c, PEG-pp-PEI-PE uncleavable/siRNA; d, PEI25K/siRNA; e, untreated cells. (C) Survivin down-regulation in A549 T24 cells analyzed by ELISA after incubation with PEG-pp-PEG-PE/anti-survivin siRNA for 48 h.

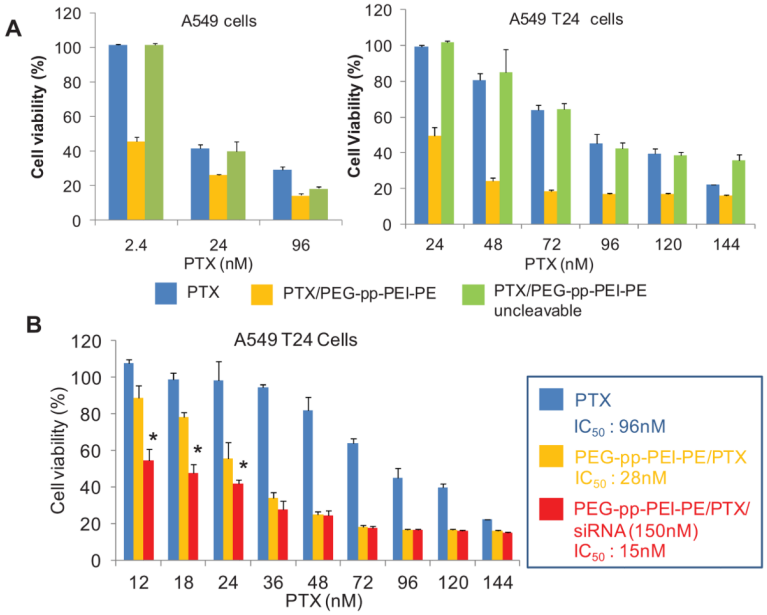

Figure 7.

Cytotoxicity analyzed by CellTiter-Blue® Cell Viability Assay. (A) Cytotoxicity of PEG-pp-PEI-PE/PTX micelles in A549 (left) and A549 T24 (right) cells; (B) Synergistic cytotoxicity of PTX and anti-survivin siRNA co-loaded nanocarriers. Incubation time: 72h.

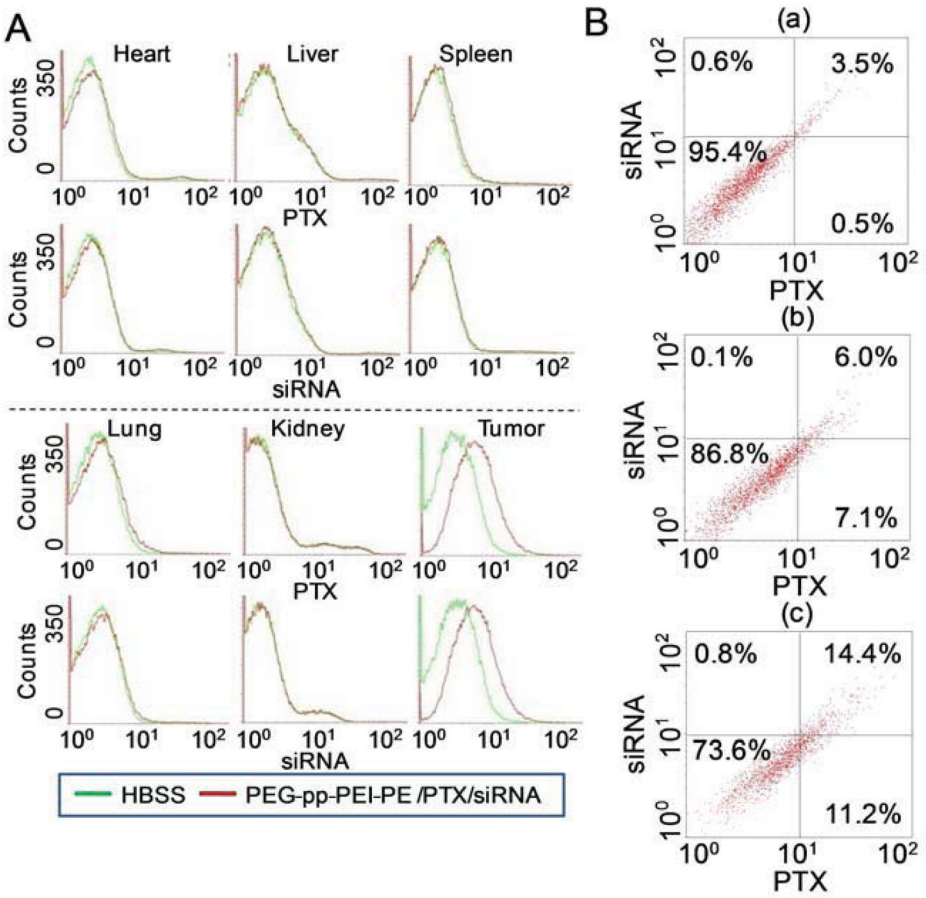

Figure 8.

In vivo co-delivery of PTX and siRNA. Oregon green-PTX and siGLO siRNA co-loaded PEG-pp-PEI-PE nanoparticles were injected intravenously in the tumor-bearing mice. At 2h post injection, the dissociated cells from fresh tissues were analyzed by FACS. (A) *In vivo* cell internalization in organ and tumor cells (histograms); (B) *In vivo* co-delivery of PTX and siRNA (dot plots). a, Untreated cells; b, PEG-pp-PEI-PE uncleavable/PTX/siRNA; c, PEG-pp-PEI-PE/PTX/siRNA.